



Received on 24 March 2014; received in revised form, 07 May 2014; accepted, 11 July 2014; published 01 October 2014

MOLECULAR MODELLING, 3D-QSAR, AND DRUG DOCKING STUDIES ON THE ROLE OF NATURAL ANTICOAGULANT COMPOUNDS IN ANTITHROMBOTIC THERAPY

Prathusha Kakarla, Amith R. Devireddy, Madhuri A. Inupakutika, Upender R. Cheeti, Jared T. Floyd, Mukherjee M. Mun, Raelyn N. Vigil, Russell P. Hunter and Manuel F. Varela *

Department of Biology, Eastern New Mexico University, Station 33, Portales - 88130, New Mexico, USA.

Keywords:

Thrombosis, Thromboembolism, Factor XIII, Antithrombotic therapy, Anticoagulants, Docking, QSAR

Correspondence to Author:

Manuel F. Varela

Professor of Biology,
Department of Biology,
Eastern New Mexico University,
Station 33, Portales - 88130, New
Mexico, USA.

E-mail: manuel.varela@enmu.edu

ABSTRACT: Thromboembolic disorders are the leading cause of human mortality. Therefore, development of effective anticoagulant therapy is critical. Factor XIIIa (FXIIIa) protein is a crucial factor in the blood coagulation cascade, and hence, it is a vital target for the evolution of new antithrombotic agents. Structure-function studies of clotting factor active sites, clot formation, and thrombus structure have gained prominence in the efforts to develop novel anticoagulants. Factor XIIIa was homology modeled with the human transglutaminase-2 crystal structure as a base template for BLAST analysis. Docking and comparative binding site analysis revealed active site residue conservation and inhibitor-protein interactions. Nineteen small molecules possessing suspected anticoagulant properties were successfully docked into the FXIIIa active site following the best CoMFA and CoMSIA prediction values. Dabigatran etexilate was anticipated to be the best FXIIIa inhibitor among the nineteen anticoagulants with the highest binding affinity for the FXIIIa protein, and the highest FlexX docks score of -29.8 KJ/mol. Structural properties of FXIIIa inhibitors with increased antithrombotic activity were predicted by this docking study.

INTRODUCTION: Many phenotypes are associated with thrombosis, and elevated levels of blood plasma coagulation factors are common ¹. Blood flow restriction due to a blockage in arteries, veins, or capillaries leads to thrombosis, a condition where a blood clot formation occurs abnormally leading to life-threatening medical manifestations. The blockade that forms as a result of the blood clot is known as a thrombus.

The thrombus can mobilize, leading to an embolism known as a thromboembolism. Embolisms can circulate all over the body, causing paralysis, sepsis, and sometimes even death ². Fibrin and platelets are crucial for the formation and stabilization of a blood clot.

Fibrin forms clots in veins whereas platelets form clots in arteries. It is well established that homozygous and heterozygous abnormalities occur at the genetic level ³⁻⁵. Thrombosis can be inherited genetically, acquired during life, or the interaction of both. According to Virchow, any obstruction in the blood flow, hypercoagulability, or injury to the blood vessel can cause venous and arterial thrombosis ⁶.

	QUICK RESPONSE CODE DOI: 10.13040/IJPSR.0975-8232.5(10).4141-52
	This article can be accessed online on www.ijpsr.com
DOI link: http://dx.doi.org/10.13040/IJPSR.0975-8232.5(10).4141-52	

Slight imbalances in the dissolution pathways of fibrin and clot formation are considered to be the main cause of thrombosis⁷. Thrombosis in its different forms like venous thrombosis, venous thromboembolism, arterial thrombosis, and pulmonary embolism cause serious life-threatening abnormalities including ischemic stroke, heart attack, deep vein thrombosis (DVT), cerebral vein thrombosis (CVT), and myocardial infarction⁸. CVT and thrombus in the blood are associated with a high mortality rate and can occur due to extremely varied causes like hypercoagulability that progresses to malignancy, homocystinemia, and an abnormality in blood coagulation⁸.

FXIII is a protein transglutaminase (TG) (PDB: 2Q3Z, www.pdb.org) (EC 2.3.2.13) that catalyzes an acyl transfer reaction. FXIII is an extracellular sulfhydrylase zymogen also known as the Laki-Lorand factor^{9,10}. Functional plasma FXIII has two B carrier subunits and two active A subunits collectively structured into a tetramer. FXIII inside the cell exists as a dimer with one A and one B subunit, both of which are produced in the bone marrow and hepatocytes, respectively. FXIII causes type-I and type-II deficiencies; type-I lacks A and B subunits, while type-II lacks the A subunit only¹¹.

Factor XIII (FXIII) levels and phenotypic polymorphisms play a major role in arterial atherothrombosis and venous thromboembolism (VTE). FXIII in its activated form, FXIIIa regulates proper clot formation and disassociation. FXIIIa 'A' chain of 626 amino acids (EC 2.3.2.13, UniProt: B4E2L8_Human, www.UniProt.org) is a fibrin-stabilizing factor (FSF), a fibrinolytic that is functional in the final stages of the blood coagulation cascade. It regulates blood homeostasis by crosslinking α and γ chain monomers forming homopolymers. FXIIIa has numerous roles in maintaining vascular permeability, in stabilizing extracellular matrix of bone and cartilage, as well as maintaining homeostasis during pregnancy, wound healing, and angiogenesis¹². In addition to its varied roles, the most important function of FXIIIa is its cardioprotective effect.

Lack of FXIIIa also leads to a rapid atrial rate enhancing the chance of stroke in the left atrium due to thrombosis, or thromboembolism¹.

Improper FXIIIa function leads to obstructive blood clots that cause microvascular thrombosis (MVT) and multi-organ dysfunction syndrome (MODS)¹³. FXIIIa inhibits thrombus formation by preventing the binding of platelets to cross-linked fibrin. There are two pathways that control blood coagulation homeostasis by regulating extrinsic and intrinsic pathways in the human body.

Thrombotic disorders are of prime concern because they account for about 500,000 deaths in Europe and up to 300,000 deaths in the United States (US) every year. Initially, heparin was the only anticoagulant prescribed in the twentieth century, but it was found to have a variety of side effects including hypersensitivity, bleeding after halting therapy, nausea, vomiting, hives, and breathing trouble¹⁴. Antithrombotic drugs function in two ways: as anticoagulants that decrease fibrin formation and as antiplatelets that inhibit clot formation by platelets¹⁵.

Anticoagulants prevent clot formation, mobilization, DVT, and PE. Hence, it is important to search for novel anticoagulant molecules. Antithrombotic therapy has been widely implemented as a remedy for conditions like DVT, CVT, and CAD. Antithrombotic therapy is also found to be effective in treating patients with heart abnormalities such as atrial fibrillation (AF) and strokes¹⁵.

In the current study, we employed molecular docking studies to elucidate the binding affinity of potential anticoagulant inhibitors to the FXIIIa active site and to provide structural evidence for blood clotting FXIIIa inhibitors to help facilitate the design of antithrombotic agents **Fig. 1**. Anticoagulants bind at the active site of FXIIIa to inhibit blood coagulation. Numbers in **Fig. 1** denote the following sequence of steps in the inhibition process.

Step 1: Catalysis and cleavage forming active peptide (P) of (4000Da) (R37-G38) and active FXIII from inactive FXIII on exposure to thrombin (T).

Step 2: Disassociation of B subunit from FXIII (B) active site (AS) in the presence of cofactor (Ca^{2+}) and amine γ glutamyl transferase (E).

Step 3a: Binding of anticoagulant molecules (AC) to the active site of FXIIIa (AS).

Step 3b: Activated FXIIIa (A) with free active site (AS) is available to crosslink fibrin monomers.

Step 4: AC changes the conformation of FXIII (A) thus out competing for fibrin and preventing blood clot formation.

Step 5: In the absence of an inhibitor, FXIIIa forms a blood clot in the presence of thrombin activation factor (Ta) and fibrin (F).

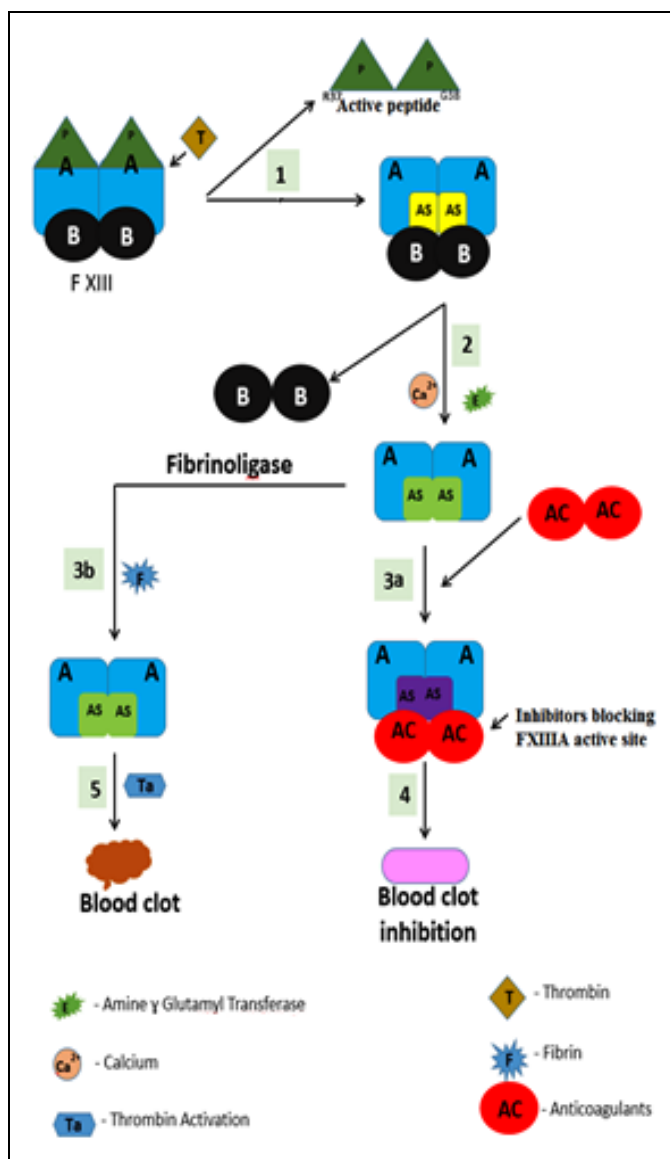


FIG. 1: MECHANISM OF FXIIIa INHIBITION BY ANTICOAGULANTS

MATERIALS AND METHODS:

Molecular Modeling: Molecular docking assists in structural molecular modeling and computer-aided drug design (CADD).

Comparative modeling was used to generate a three dimensional (3D) structure for human FXIIIa (UniProt ID: B4E2L8) blood coagulation protein to provide structural data on ligand-protein complexes and to analyze the interactions at the molecular level. The homodimer crystal structure of the human transglutaminase-2 (PDB code: 2Q3Z) was used as a base template to construct the 3D model of FXIIIa.

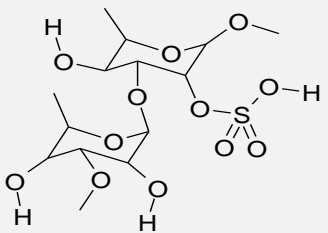
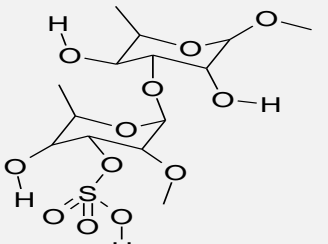
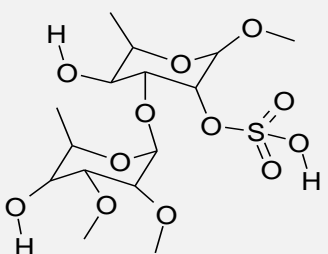
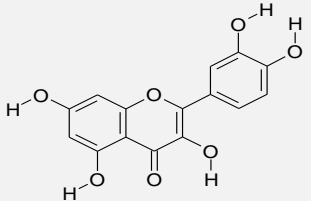
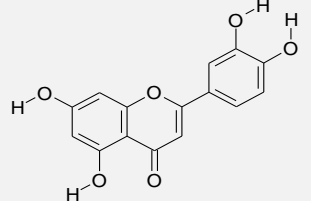
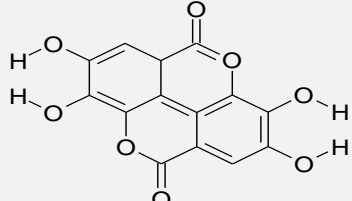
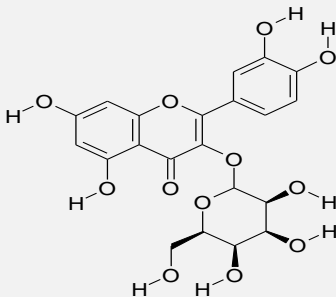
Sequence alignment for both the query and the template sequences was performed using ClustalX analyzer, and Modeller 9.10 software was utilized to construct 3D models, and SPDBV software was used to perform loop building of amino acid residues that exist in disallowed regions.

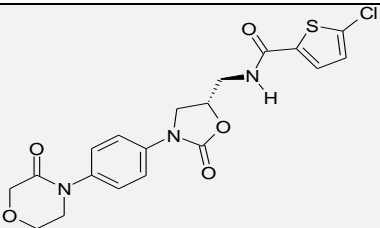
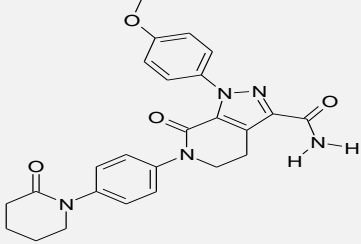
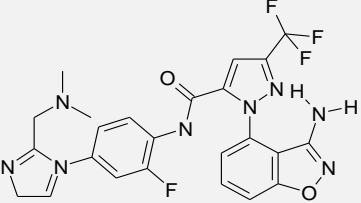
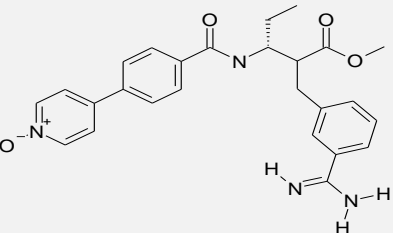
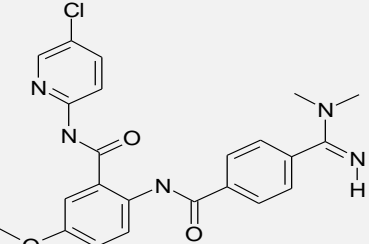
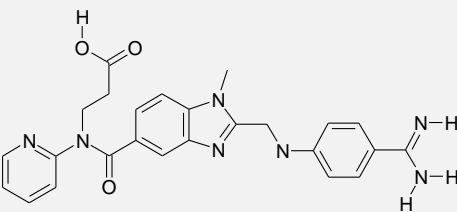
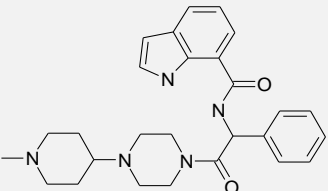
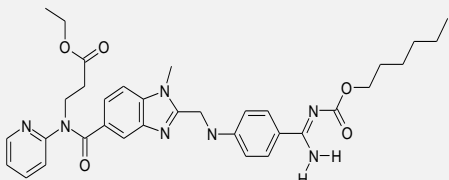
Energy minimized 3D model was generated through SYBYL 6.7 (FlexX) software using default parameters of Tripos force field engine with distance-dependent dielectric function by applying Gasteiger-Huckel partial atomic charges¹⁶⁻¹⁸. This energetically favorable model generated was stereochemically evaluated using SPDBV software. Ramachandran plot phi (ϕ) and psi (ψ) values were determined using PROCHECK v 3.4.4.

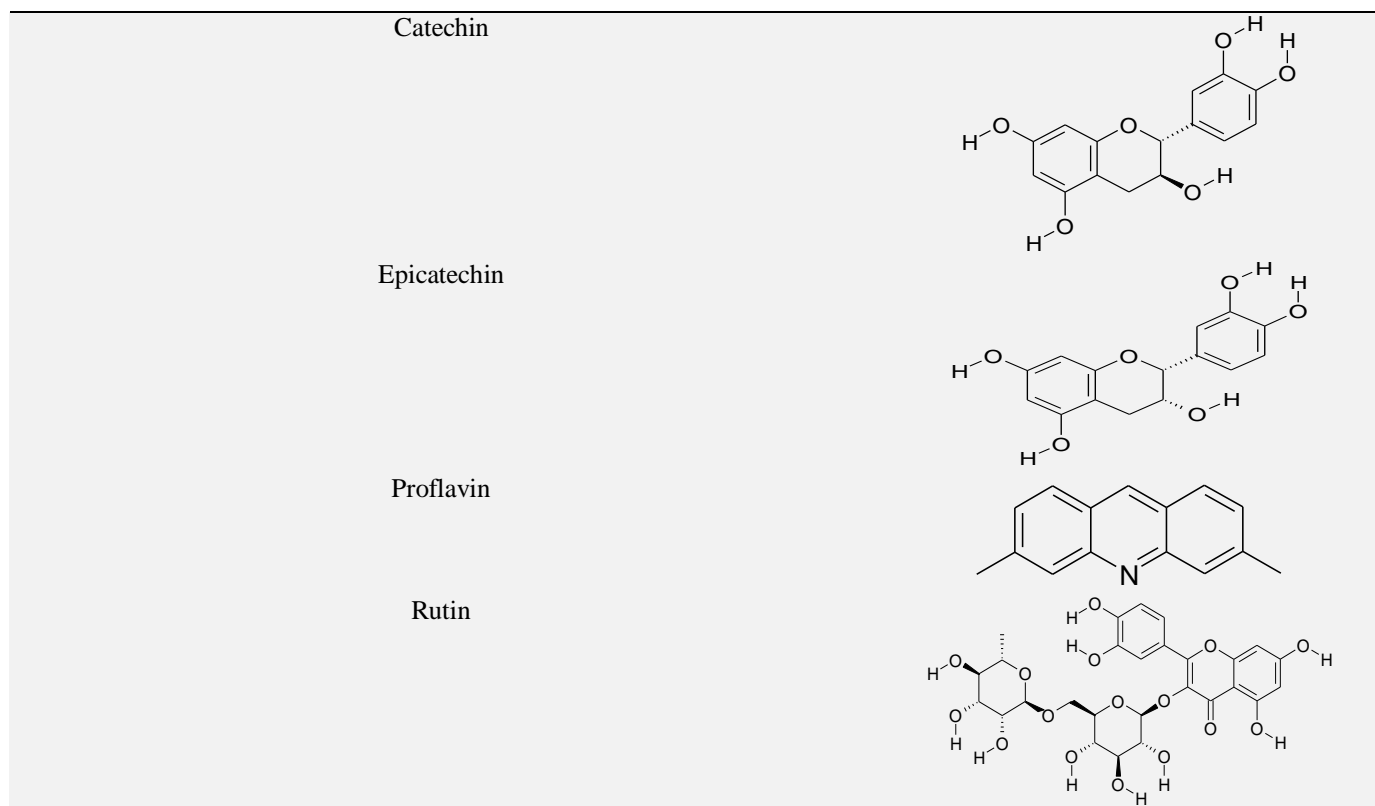
Geometry Optimization and Molecular Docking: Protein-ligand binding exhibits high specificity and is very important for many biological processes. FlexX interfaced with SYBYL 6.7 was employed to estimate binding interactions by docking a set of 19 anticoagulant compounds into the active site of the FXIIIa. In SYBYL 6.7, the flexibility of ligands is considered while the protein is considered as a rigid structure. In this automated program, each new fragment is added to the base fragment in all possible angles and confirmations at the active site.

Nineteen natural compounds with anticoagulant property were selected from an earlier report and employed in this study. pIC₅₀ (-log IC₅₀) values for all the compounds were derived from IC₅₀ and biological activity data reported in the literature¹⁹⁻²². Chemical structures of these 19 small compounds exhibiting anticoagulant activity were drawn in SYBYL and were geometrically optimized using default parameters and convergence criterion of 0.001 kcal/mol **Table 1**²³.

TABLE 1: CHEMICAL STRUCTURE OF NINETEEN ANTICOAGULANT MOLECULES DRAWN AND GEOMETRICALLY OPTIMIZED IN SYBYL 6.7

Compound	Structure
$\rightarrow 3\text{-}\alpha\text{-L-Rhamnopyranose-2-sulfate-(1}\rightarrow 3\text{)-}\alpha\text{-L-Rhamnopyranose-(1}\rightarrow$	
$\rightarrow 3\text{-}\alpha\text{-L-Rhamnopyranose-(1}\rightarrow 2\text{)-}\alpha\text{-L-Rhamnopyranose-3-sulfate-(1}\rightarrow$	
$\rightarrow 3\text{-}\alpha\text{-L-Rhamnopyranose-2-sulfate-(1}\rightarrow 2,3\text{)-}\alpha\text{-L-Rhamnopyranose-(1}\rightarrow$	
Quercetin	
Luteolin	
Ellagic acid	
Hyperosid	

Rivaroxaban	
Apixaban	
Razaxaban	
Otamixaban	
Betrixaban	
Dabigatran	
Ly-517717	
Dabigatran etexilate	



SYBYL 6.7 interfaced with the FlexX fast; automated docking program was used to trace out the probable binding conformations of these 19 inhibitors around an active radius of 6.5\AA ¹⁷. Default FlexX docking parameters were employed to obtain the docking scores. Binding interactions were further examined based on the best-docked conformation. Information on the structure and energetics of molecular complexes were obtained using SYBYL-FlexX.

Structure and Activity Relationship (SAR)

Studies: Three-dimensional quantitative structure-activity relationship (QSAR) studies based on comparative molecular field analysis (CoMFA), and molecular similarity indices in comparative analysis (CoMSIA) methods were carried out for the set of 19 molecules to determine their activity as potential antithrombotic agents. CoMFA utilizes tripos force field with a distance-dependent dielectric constant in all interactions in a regularly spaced (2×10^{-10} m) grid taking an sp^3 carbon atom as a steric probe and a +1 charge as an electrostatic probe. The cut-off was set to 30 kcal mol⁻¹. CoMSIA utilizes Gaussian-type distance-dependent dielectric constant to minimize changes in atomic positions and charge potentials at the grids. CoMSIA calculates using a C+ probe atom with a

radius of 1×10^{-10} m placed at a regular grid spacing of 2×10^{-10} m to enclose all the binding conformations of the inhibitors. The pIC₅₀ data will couple 3-log units offering a wide and similar set of data for 3D-QSAR analysis. Compounds were divided into test and training set in a 1:3 ratio to improve the predictivity of the 3D-QSAR models. Cross-validation and partial least score (PLS) analyses were used where the cross-validated coefficient (q^2) leaving an optimal number of components and lowest standard error of prediction was considered for the accuracy determination of the predicted models²⁴.

RESULTS AND DISCUSSION:

The Molecular Modeled Protein showed an Effective 3D Structural Conformation with PROCHECK Analysis: The final model generated in this study was evaluated using PROCHECK. Ramachandran plot results **Fig. 2** emphasized that 87.1% of the amino acids were located in the most favored region, and approximately 12.2% and 0.5% of amino acids were located in allowed and generously allowed regions, respectively. Only one amino acid (Leu-377) was in the disallowed region, suggesting a better structural conformation than the base template **Fig. 3**.

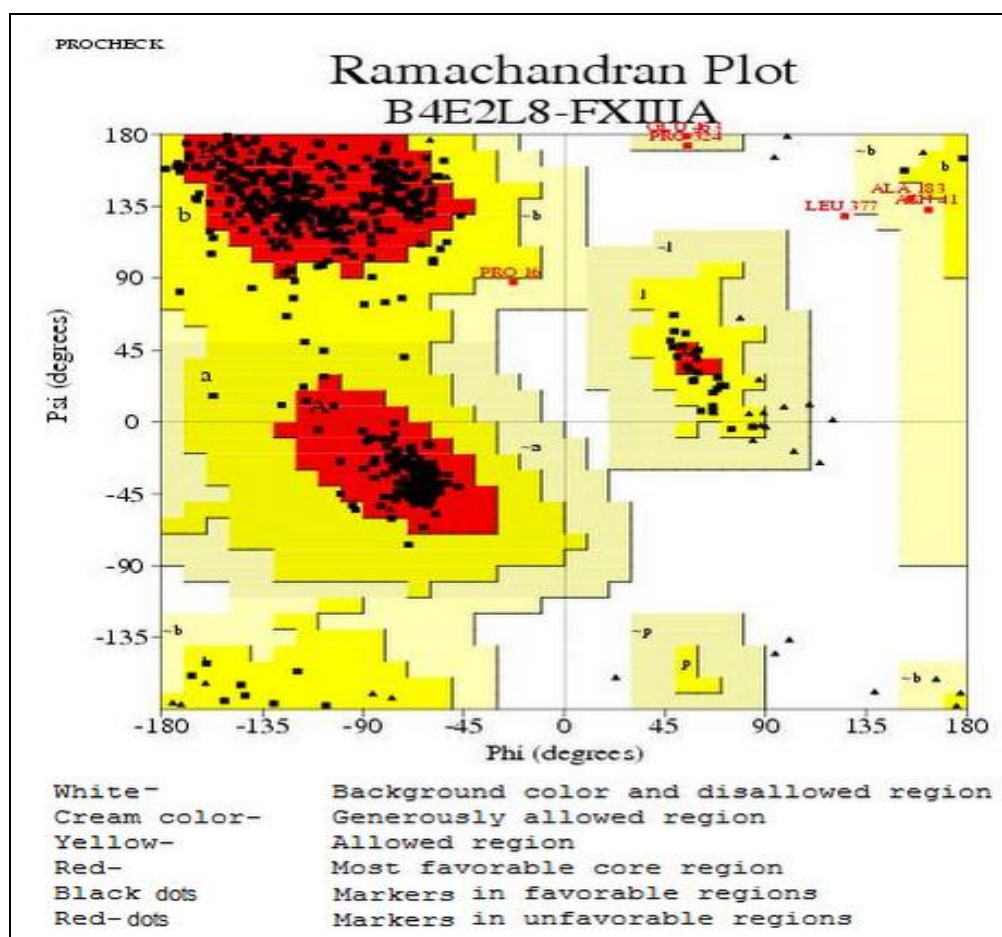


FIG. 2: RAMACHANDRAN PLOT OF (B4E2L8) FXIII A WITH PSI/PHI VALUES CALCULATED BY PROCHECK PROGRAM

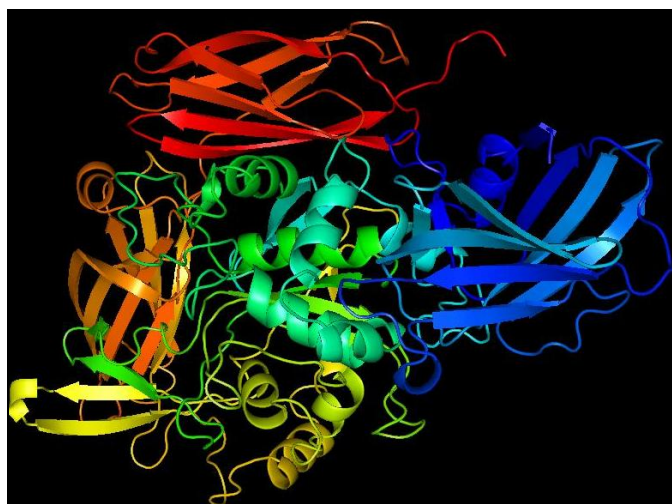


FIG. 3: SECONDARY STRUCTURAL CONFORMATION OF B4E2L8- FXIII A PROTEIN

Highest FlexX Dock Score and Amino Acid Interactions Revealed the Inhibitory Potential of Anticoagulants at the FXIII A Active Site:

Current molecular docking simulation studies on natural anticoagulant molecules and FXIII A predict a significant correlation in the docking scores obtained.

The observation that many polar residues in the FXIII A binding pocket form hydrogen bond interactions with the anticoagulant molecules were revealed in this docking study. The FlexX dock scores and hydrogen binding interactions of all the 19 anticoagulant compounds with the active site are tabulated in **Table 2**. Most of the crucial active site residues of FXIII A were found to hold significant hydrogen binding interactions with a good FlexX dock score to indicate binding. Among the 19 anticoagulant molecules docked to FXIII A: dabigatran etexilate **Fig. 4**, dabigatran **Fig. 5**, rivaroxaban **Fig. 6**, and betrixaban **Fig. 7** were found to be the most potentially active compounds exhibiting a FlexX dock score of -29.8 KJ/mol, -28.5 KJ/mol, -27.2 KJ/mol, -27.9 KJ/mol, respectively. Hyperosid **Fig. 8**, dabigatran etexilate **Fig. 4**, and catechin **Fig. 9** had the highest number of interactions with the active site of FXIII A. Dabigatran etexilate shown in **Fig. 4** had the best docking score of -29.8 KJ/mol as well as the highest number of amino acid interactions with the FXIII A active site.

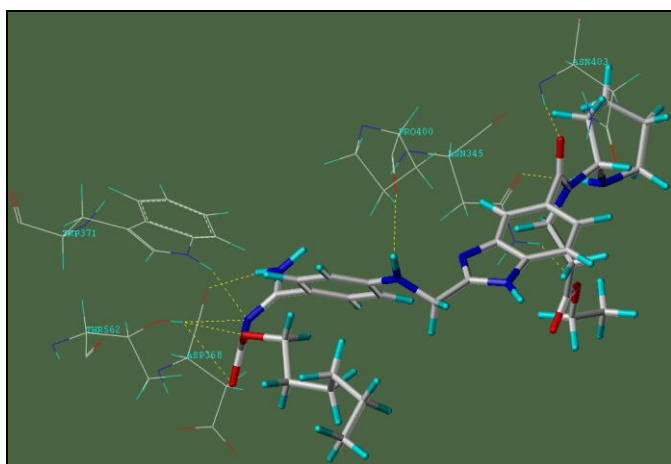


FIG. 4: DABIGATRAN ETEXILATE EXHIBITING FLEXX DOCK SCORE OF -29.8 KJ/MOL. Structure in the ball-and-stick model represent dabigatran etexilate and in lines represents FXIIIa protein.

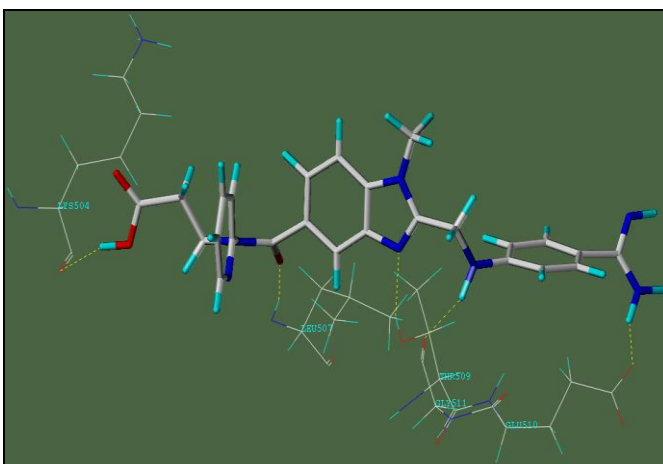


FIG. 5: DABIGATRAN EXHIBITING FLEXX DOCK SCORE OF -28.5 KJ/MOL. Structure in the ball-and-stick model represent dabigatran and in lines represents FXIIIa protein.

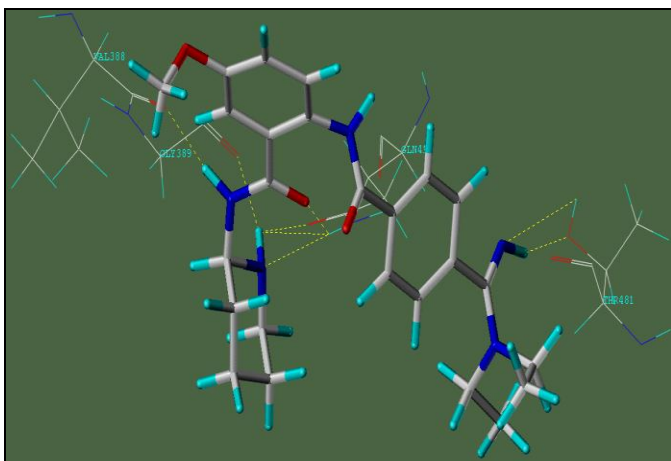


FIG. 6: BETRIXABAN EXHIBITING FLEXX DOCK SCORE OF -27.9 KJ/MOL. Structure in the ball-and-stick model represent betrixaban and in lines represents FXIIIa protein.

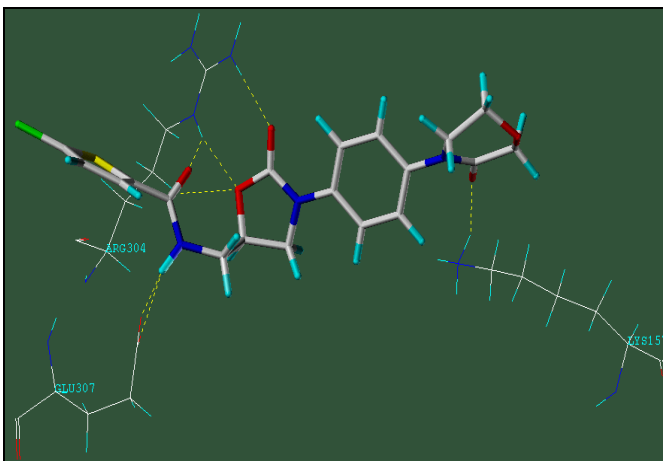


FIG. 7: RIVAROXABAN EXHIBITING FLEXX DOCK SCORE OF -27.2 KJ/MOL. Structure in the ball-and-stick model represent rivaroxaban and in lines represents FXIIIa protein.

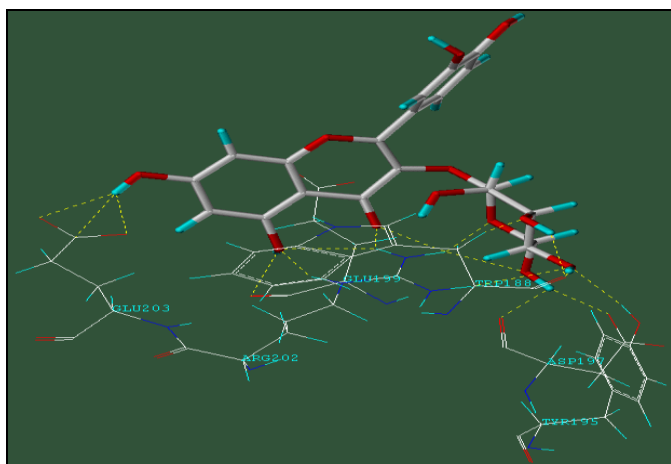


FIG. 8: HYPERSOID SHOWING 6 HIGHEST NUMBERS (YELLOW LINES) OF AMINO ACID INTERACTIONS (GLU-203, ARG-202, GLU-199, TRP-188, ASP-197, TYR-195) WITH FXIIIa ACTIVE SITE. Structure in the ball-and-stick model represent hypersoid and in lines represents FXIIIa protein.

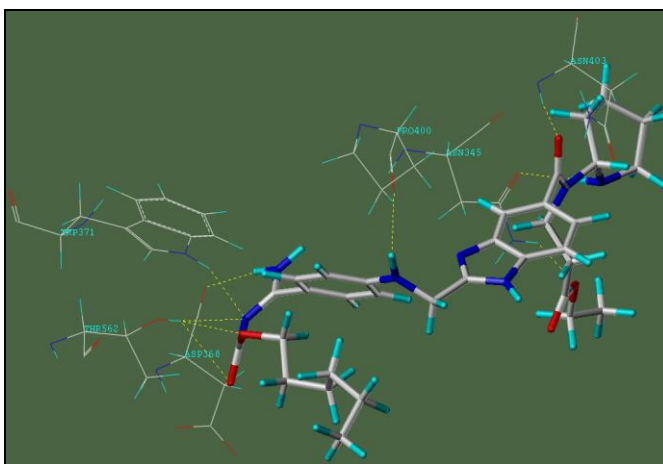


FIG. 9: CATECHIN SHOWING 6 AMINO ACID INTERACTIONS (YELLOW LINES) WITH THE ACTIVE SITE OF FXIIIa (TRP-371, THR-562, ASP-368, PRP-400, ASN-345, ASN-403). Structure in the ball-and-stick model represent catechin and in lines represents FXIIIa protein.

The 19 molecules docked into the active site of blood coagulation FXIIIa protein (B4E218) exhibited consistent amino acid interactions. The FlexX dock scores with interactions of the residues and their distance from the FXIIIa active protein to the anticoagulant ligands are indicated in **Table 2**.

TABLE 2: FLEXX DOCK SCORES, INTERACTING AMINO ACIDS OF ANTICOAGULANTS, AND THEIR DISTANCE FROM FXIIIa

Compound	Interacting amino acids list	Number of Interactions	Distance (Å) between interacting amino acid and anticoagulants	Dock score (KJ/mol)
Dabigatran etexilate	Asn-403	6	1.9	-29.8
	Asn-345		1.866, 1.911	
	Asp-368		1.834	
	Thr-562		2.705, 2.713, 2.199	
	Trp-371		2.091	
	Pro-400		2.154	
Dabigatran	Lys-504	5	2.168	-28.5
	Leu-507		1.698	
	Glu-510		1.577	
	Thr-509		2.21	
	Gly-511		1.896	
Betrixaban	Val-388	4	2	-27.9
	Gly-389		2.144	
	Gln-416		2.192, 2.211, 2.152, 2.148	
	Thr-481		2.710, 1.640	
Rivaroxaban	Lys-157	3	1.965	-27.2
	Glu-307		1.845, 2.261	
	Arg-304		2.218, 2.228, 2.688, 2.099, 2.510	
Razaxaban	Ile-630	3	1.587, 2.360	-25
	Ile-633		1.691, 2.719	
	Tyr-719		1.962	
Quercetin	Asp-244	5	2.211	-24.8
	Asn-308		2.167	
	Glu-307		1.911	
	Gly-274		2.083	
	Tyr-303		1.413, 2.356, 1.773	
Apixaban	Arg-59	3	2.206	-23
	Trp-58		1.927	
	Lys-74		2.091	
Ellagic acid	Arg-697	5	2.086	-22.5
	Val-673		2.537	
	Gly-672		2.052	
	Asp-233		2.445, 2.041	
	Thr-674		2.531, 1.631	
Luteolin	Tyr-442	5	1.664, 2.187	-22.3
	Asp-352		1.757, 2.403, 2.440	
	Gly-502		2.236, 2.524	
	Ala-503		2.023	
	Lys-504		1.725	
Ly-517717	Tyr-168	4	1.81	-22.3
	Arg-96		1.710, 2.065, 1.828	
	Arg-97		1.995	
	Asp-98		2.641, 1.790, 2.604	
Catechin	Lys-270	4	2.586	-20
	Pro-400		1.781	

	His-343	6	1.947	
	Trp-371		2.338, 2.305	
	Thr-562		2.005	
	Gly-278		2.186, 2.061, 2.212	
Hyperosid	Glu-203		2.056, 2.067, 2.334	
	Glu-199		2.122	
	Arg-202	6	2.085, 2.390, 0.981, 2.147, 2.509,	-19.6
			2.036, 2.599	
	Asp-197		1.931, 2.053	
	Tyr-195		2.07	
	Trp-188		2.114, 2.157, 2.228	
Rutin	Asp-723	4	1.837, 1.801	-19.4
	Gln-725		2.283, 1.578, 1.945	
	Gln-641		1.456, 1.871	
	Gln-727		1.713	
→3-α-L-Rhamnopyranose-	Asp-197		2.192, 1.921, 2.176	
2-sulfate-(1→2,3)- α-L-	Tyr-195	5	2.504	-18.8
Rhamnopyranose-(1→	Glu-199		2.186, 2.140	
	Arg-202		1.838, 2.094	
	Trp-188		1.674	
Epicatechin	Lys-504			
	Met-500		1.779	-18.2
	Gln-350	5	2.257, 2.601	
	Asn-348		1.824	
	Leu-349		1.749	
→3-α-L-Rhamnopyranose-	Asp-64		2.312	
2-sulfate-(1→3)- α-L-	Trp-188	5	2.670, 1.749	-17.6
Rhamnopyranose-(1→	Asp-197		2.348	
	Tyr-195		2.09	
	Arg-202		2.180, 1.497	
Proflavin	Pro-656	2	1.937	-17.1
	Lys-658		1.946	
→3-α-L-Rhamnopyranose-	Thr-393		2.449, 2.345, 2.223, 2.129	
(1→2)- α-L-	Glu-201	4	1.1571, 1.535, 1.694	-17
Rhamnopyranose-3-sulfate-	Thr-481		1.58	
(1→	Glu-416		2.522, 2.331, 2.393, 1.900, 1.826, 2.047	
Otamixaban	Ser-306		2.701	
	Glu-307	5	2.194	-12.7
	Tyr-241		2.118	
	Tyr-109		1.904	
	Arg-108		1.887, 1.852	

Quantitative Structure-Activity Relationship Study (QSAR) Results Indicate a Better Fit Between FXIIIa and the Anticoagulants, and PLS Statistical Analysis Supports the Accuracy of Predicted and Docked Models: CoMFA and CoMSIA studies support the accuracy of predicted and docked models. PLS, the statistical analysis with multivariate regression and LOO cross-validated PLS analysis was employed to deduce the 3D QSAR models. Employing default SYBYL

CoMSIA and CoMFA parameters on all the 19 compounds set with the multifit molecular alignment resulted in a PLS model with average q^2 values, r^2 values, SEE , and F -values **Table 3**. These results signify stability and robustness in the CoMFA and CoMSIA QSAR models, confirming the structural and functional relationships of docked FXIIIa with those of anticoagulant molecules indicating a good protein-ligand fit **Table 3**.

TABLE 3: PLS STATISTICS OF COMFA AND COMSIA, 3D- QSAR MODELS OBTAINED FROM DOCK ALIGNMENT

Fields	CoMFA	CoMSIA
q^2	0.609	0.596
r^2	0.938	0.945
SEE	0.157	0.151
F	131.708	126.628

q^2 - loo-cross-validated correlation coefficient; r^2 - non-cross-validated correlation coefficient, n- Number of components used in PLS analysis, SEE- standard error estimation, F value- Fischer ratio values for all the nineteen molecules validated as test and training set confirms that these models have the best predictivity

CONCLUSION: *In-silico* comparative 3-dimensional modeling and structure-activity relationship studies on anticoagulant FXIIIa inhibitor molecules are increasingly prominent because of their potency to act against thrombosis.

The anticoagulants tested in the current study illustrate the mechanism of small molecules that form bonds with the active site of FXIIIa, making them unavailable to trigger the blood coagulation cascade. We have predicted these natural compounds to be the best antithrombotic drug candidates because of their strong affinities with the active site of the FXIIIa.

Furthermore, *in-vivo* studies performed employing antithrombotic therapy using this information as a base will aid in the elucidation of therapy that is specific to thrombosis.

ACKNOWLEDGEMENT: This work was made possible by the NM-INBRE program grant P20GM103451 from the National Center for Research Resources. This publication was also supported by an internal research grant awarded by the Department of Biology, Eastern New Mexico University, Portales, New Mexico, USA.

CONFLICT OF INTEREST: Nil

REFERENCES:

- Lim HS: Effect of atrial fibrillation on atrial thrombogenesis in humans: impact of rate and rhythm. *J Am Coll Cardiol* 2013; 61(8): 852-60.
- Hong KC: Risk factors and incidence of deep vein thrombosis in lower extremities among critically ill patients. *J Clin Nurs* 2012; 21(13-14): 1840-6.
- Tang, L: PROC c.574_576del polymorphism: a common genetic risk factor for venous thrombosis in the Chinese population. *J Thromb Haemost* 2012; 10(10): 2019-26.
- Antalfi, B: Factor XIII-A subunit Val34Leu polymorphism in fatal hemorrhagic stroke. *Int J Lab Hematol* 2013; 35(1): 88-91.
- Berezky Z and Muszbek L: Factor XIII and venous thromboembolism. *Semin Thromb Hemost* 2011; 37(3): 305-14.
- Boehlen F: Acquired factor XIII deficiency: a therapeutic challenge. *Thromb Haemost* 2013; 109(3): 479-87.
- Meetoo D: In too deep: understanding, detecting and managing DVT. *Br J Nurs* 2010; 19(16): 1021-7.
- Ruiz-Sandoval JL: Cerebral venous thrombosis in a Mexican multicenter registry of acute cerebrovascular disease: the RENAMEVASC study. *J Stroke Cerebrovasc Dis* 2012; 21(5): 395-00.
- Kohler HP: Diagnosis and classification of factor XIII deficiencies. *J Thromb Haemost* 2011; 9(7): 1404-6.
- Katona E: Measurement of factor XIII activity in plasma. *Clin Chem Lab Med* 2012; 50(7): 1191-02.
- Izumi T: Type I factor XIII deficiency is caused by a genetic defect of its b subunit: insertion of triplet AAC in exon III leads to premature termination in the second Sushi domain. *Blood* 1996; 87(7): 2769-74.
- Hsieh L and Nugent D: Factor XIII deficiency. *Haemophilia* 2008; 14(6): 1190-00.
- Semeraro CTAN, Semeraro F and Colucci M: Sepsis, thrombosis and organ dysfunction. *Thrombosis Research* 2011; 129(3): 290-95.
- Neishi Y, Okura H and Yoshida K: Deep Vein Thrombosis Caused by Heparin-induced Thrombocytopenia Thrombosis. *Internal Medicine* 2013; 52(8): 929-29.
- Bates SM: Diagnosis of DVT: Antithrombotic Therapy and Prevention of Thrombosis, 9th ed: American College of Chest Physicians Evidence-Based Clinical Practice Guidelines. *Chest* 2012; 141(2 S): e351S-418S.
- Gasteiger J and Marsili M: Iterative partial equalization of orbital electronegativity - rapid access to atomic charges. *Tetrahedron* 1980; 36(22): 3219-28.
- Dolan MA, Keil M and Baker DS: Comparison of composer and ORCHESTRAR. *Proteins: Structure, Function, and Bioinformatics* 2008; 72(4): 1243-58.
- Tsai KC: A comparison of different electrostatic potentials on prediction accuracy in CoMFA and CoMSIA studies. *Eur J Med Chem* 2010; 45(4): 1544-51.
- Li H: Structural characterization of an anticoagulant-active sulfated polysaccharide isolated from green alga *Monostroma latissimum*. *Carbohydrate Polymers* 2011; 85(2): 394-00.
- Remko M: Molecular structure, lipophilicity, solubility, absorption, and polar surface area of novel anticoagulant agents. *Journal of Molecular Structure: THEOCHEM* 2009; 916(1-3): 76-85.
- Correia-da-Silva M: Dual anticoagulant/antiplatelet persulfated small molecules. *Eur J Med Chem* 2011; 46(6): 2347-58.
- Gunda SK, Kakarla P and Shaik M: Molecular Modelling and Docking Studies of Human Blood Coagulation Factor-XIIIa Protein. *International Journal of Research in Pharmaceutical and Biomedical Sciences* 2013; 4(2): 647-55.
- Wasay M: Predictors of cerebral venous thrombosis and arterial ischemic stroke in young Asian women. *J Stroke Cerebrovasc Dis* 2012; 21(8): 689-94.

24. Stoyanova-Slavova IB: Partial least square and k-nearest neighbor algorithms for improved 3D quantitative spectral

data-activity relationship consensus modeling of acute toxicity. *Environ Toxicol Chem* 2014; 33(6): 1271-82.

How to cite this article:

Kakarla P, Devireddy AR, Inupakutika MA, Cheeti UR, Floyd JT, Mun MM, Vigil RN, Hunter RP and Varela MF: Molecular modelling, 3d-qsar, and drug docking studies on the role of natural anticoagulant compounds in antithrombotic therapy. *Int J Pharm Sci & Res* 2014; 5(10): 4141-52. doi: 10.13040/IJPSR.0975-8232.5(10).4141-52.

All © 2013 are reserved by International Journal of Pharmaceutical Sciences and Research. This Journal licensed under a Creative Commons Attribution-NonCommercial-ShareAlike 3.0 Unported License.

This article can be downloaded to **ANDROID OS** based mobile. Scan QR Code using Code/Bar Scanner from your mobile. (Scanners are available on Google Playstore)